Antenna Arrays

Recall from our previous discussion of the 2-element array that the total field pattern from an array could be found by multiplying the element factor (the pattern produced by a single element) by the array factor. We found that that array factor represents the response of an array of isotropic elements, allowing us to treat the element and the array separately.

We now consider more general examples of arrays. First, we will consider arrays with any number of elements. Then, we will consider the case where the elements are not necessarily excited by the same signal, but excited by signals with different amplitudes and/or phases.

1 Array Factor for N Elements

Consider a single isotropic radiator that has a radiated field that is proportional to

$$\frac{e^{-jkr}}{4\pi r}. \tag{1}$$

Hence, the radiation intensity associated with this is constant (isotropic). We can write the unnormalized array factor of such a situation as

$$AF = 1 \tag{2}$$

Now consider the array shown in Figure 1, which is receiving a signal from a plane wave incident at angle θ to the plane of the array.

Each element is excited with a signal at an amplitude of 1, but because the transmission paths between elements are not equal, the phase shift of each element will be different. Hence, we can write the array factor as

$$AF = e^{j\xi_0} + e^{j\xi_1} + e^{j\xi_2} + \cdots + e^{j\xi_{N-1}} \tag{3}$$

where ξ_m are the phases of an incoming plane wave at the element locations $m = 0, 1, \ldots$, referenced to some point such as the origin. Hence, the phase of the wave arriving at element m leads the phase of the wave arriving at the origin by ξ_m.

Now we consider the case where all the array elements are separated by the same distance d, leading to a linear array of total length $D = (N-1)d$. Such an array is called an *equally spaced linear array* (ESLA), and since the excitation is uniform, we called it a uniformly excited ESLA. The geometry of the array then resembles the figure shown in Figure 1.

From the figure, we can see that the phase of element $m+1$ leads that phase of element m by $kd\cos\theta$, since the path length to element $m+1$ is $d\cos\theta$ metres longer than that to m. If we arbitrarily set the reference point to element 0, so that $\xi_0 = 0$, we can write the array factor[1] as

$$AF = 1 + e^{jkd\cos\theta} + e^{jk2d\cos\theta} + \cdots e^{jk(N-1)d\cos\theta} \tag{4}$$

$$= \sum_{m=0}^{N-1} e^{jkmd\cos\theta} = \sum_{m=0}^{N-1} e^{jkm\frac{d}{N-1}\cos\theta} \tag{5}$$

[1] Note the Balmain notes use indices starting at 1, so $m = n - 1$

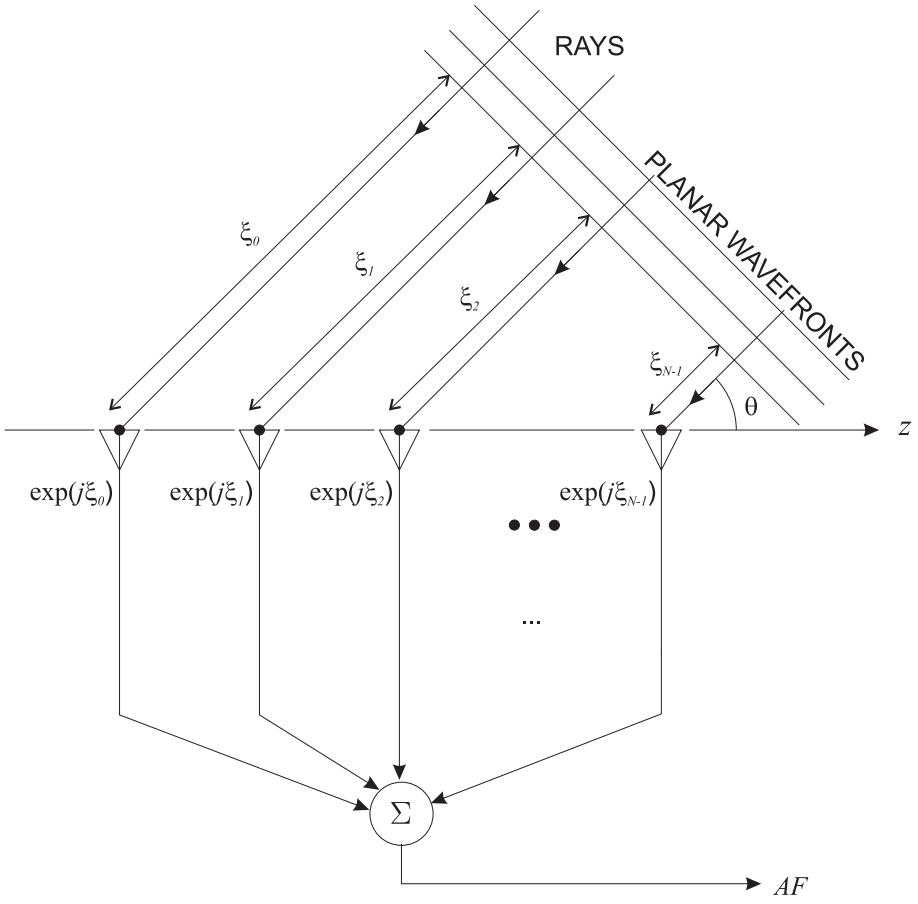

Figure 1: Ray diagram for linear receiving array

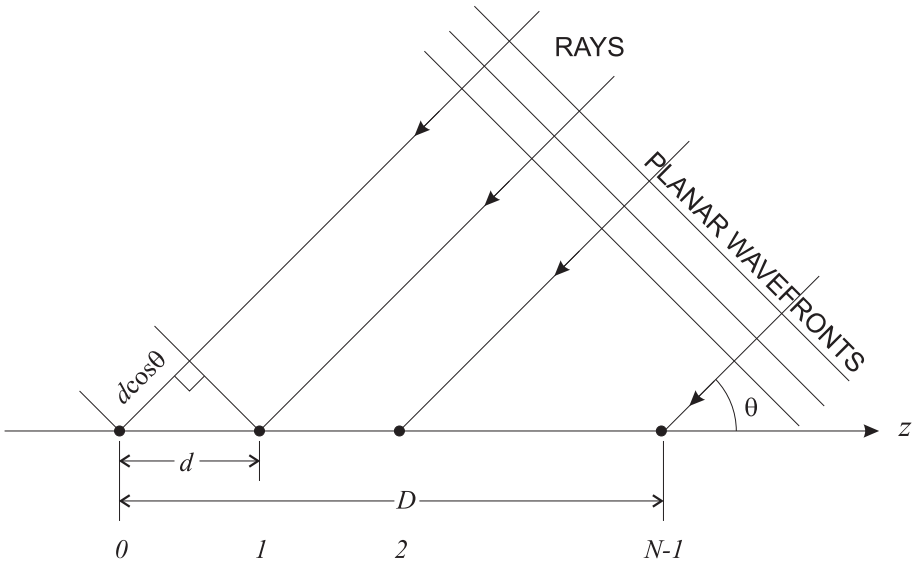

Figure 2: Linear array geometry

Defining

$$\psi = kd\cos\theta, \tag{6}$$

the expression for array factor becomes

$$AF = \sum_{m=0}^{N-1} e^{jm\psi} = 1 + e^{j\psi} + e^{j2\psi} + \cdots + e^{j(N-1)\psi} \tag{7}$$

This function is a function of ψ and resembles a Fourier Series where the array factor is composed of a set of sinusoids at multiples of a 'fundamental frequency' ψ. More on this later.

Note that because of reciprocity, the array works similarly in transmit mode except the direction of the phase gradient is reversed to produce a plane wave leaving the array in the direction shown.

2 Plotting the Array Factor

It is not obvious what the radiation pattern produced by the array factor looks like by examining Equation (7). Here we will present a simple graphical procedure for plotting the array factor. Let's multiply Equation (7) by $e^{j\psi}$ to obtain

$$AF \cdot e^{j\psi} = e^{j\psi} + e^{j2\psi} + e^{j3\psi} + \cdots + e^{jN\psi} \tag{8}$$

Subtracting Equation (8) from Equation (7) results in

$$AF(1 - e^{j\psi}) = 1 - e^{jN\psi}. \tag{9}$$

Rearranging,

$$\begin{aligned} AF &= \frac{1 - e^{jN\psi}}{1 - e^{j\psi}} && (10)\\ &= \frac{e^{jN\psi/2}}{e^{j\psi/2}} \frac{e^{jN\psi/2} - e^{-jN\psi/2}}{e^{j\psi/2} - e^{-j\psi/2}} && (11)\\ &= e^{j(N-1)\psi/2} \frac{\sin(N\psi/2)}{\sin(\psi/2)} && (12) \end{aligned}$$

The maximum value of AF occurs when $\psi = 0$, resulting in $AF = N$. Therefore, disregarding the phase factor and normalizing we obtain

$$f(\psi) = \frac{\sin(N\psi/2)}{N\sin(\psi/2)} \tag{13}$$

To plot the array factor, we note that Equation (6) defines the polar equation of a circle, and is used to relate ψ to θ. Let's take an example for the 2-element case we have already discussed earlier, and set the array spacing to $d = \lambda/2$.

To plot the radiation pattern pattern as a function of θ, we plot $|f(\psi)|$ and a circle of radius $\psi = kd = \frac{2\pi}{\lambda}\frac{\lambda}{2} = \pi$ below the plot, as shown in the illustration in Figure 2. Then, by sweeping

θ from $-\pi$ to π, we trace out the projected array pattern inside the circle as follows. For a given angle θ, determine the point of intersection of a radial line from the origin with the perimeter of the circle. Then draw a vertical line up from this point and determine the value of $f(\psi)$ at this point. Since the circle has radius 1, which is the maximum value of $|f(\psi)|$, the projection of the point back inside the circle is at a distance $|f(\psi)|$ from the origin. This is repeated for as many points as necessary to construct the radiation pattern.

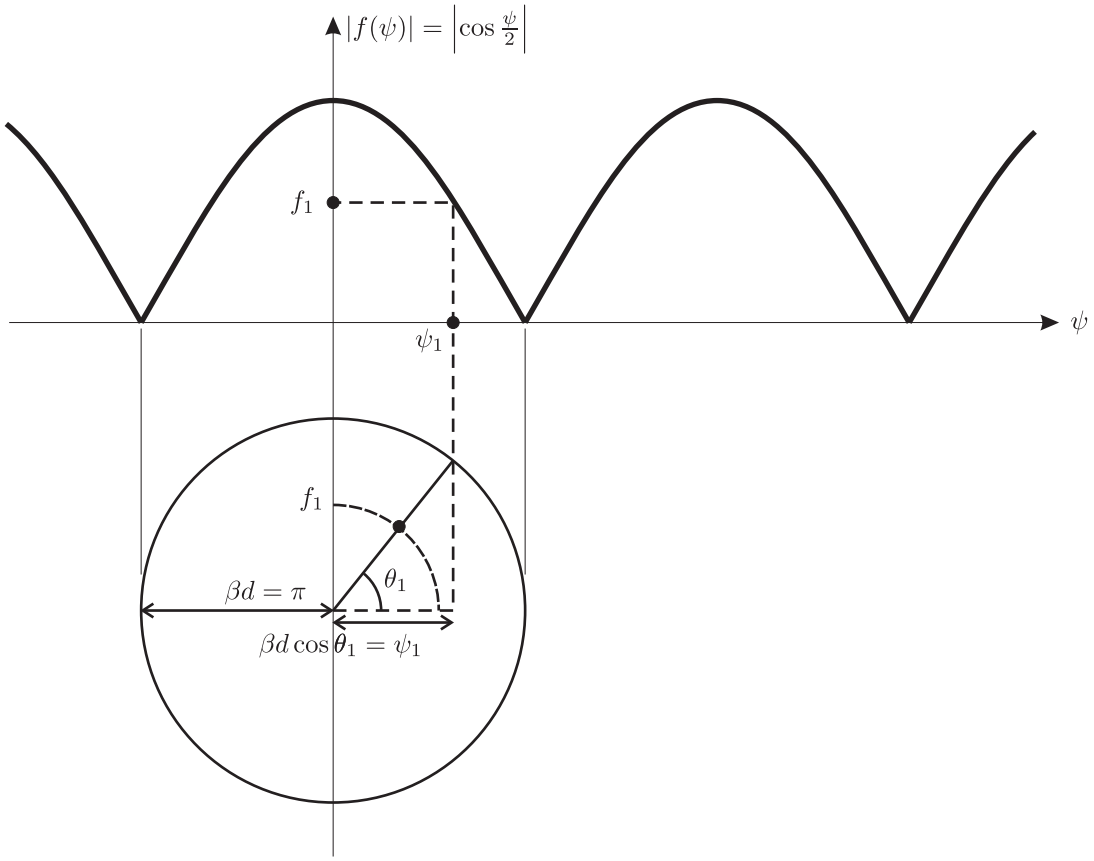

Figure 3: Geometric array factor construction

The region $-1 < \cos\theta < 1$ or $-kd < kd\cos\theta < kd$, or the horizontal extent of the circle, is known as the *visible region*, since $|f(\psi)|$ is only evaluated for ψ values in this region.

Evaluating $|f(\psi)|$ for various values of N yields the curves shown in Figure 2. The exact shape of the radiation pattern depends on the size of the visible region, but we can may several important observations about this plot.

1. There is always a maximum at $\psi = 0$, corresponding to $\theta = 90°$, which is called the *broadside direction* as it is normal to the plane of the array.

2. As N increases, the width of the main lobe decreases. In fact, the first null beamwidth can be found by considering where the numerator of Equation (13) go to zero, or where

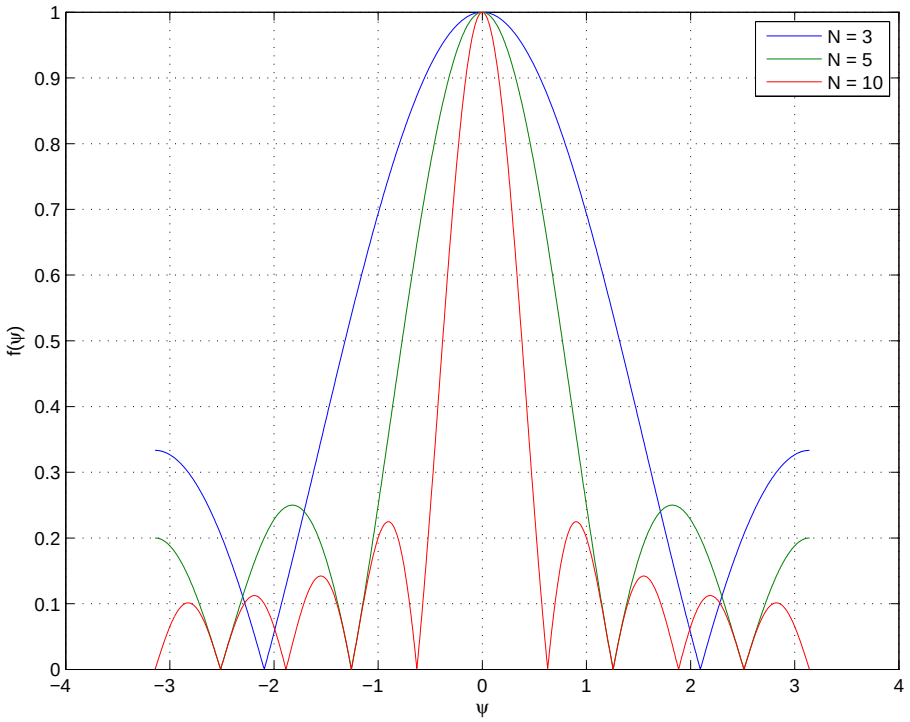

Figure 4: Plots of $|f(\psi)|$ for various N

$N\psi_{FN}/2 = \pm\pi \Rightarrow \psi_{FN} = \pm 2\pi/N$. Since $\psi = kd\cos\theta$,

$$\pm\frac{2\pi}{N} = \frac{2\pi}{\lambda} d\cos\theta_{FN} \tag{14}$$

$$\theta_{FN} = \cos^{-1}\left(\pm\frac{\lambda}{Nd}\right) \tag{15}$$

The first null beamwidth is then found as

$$FNBW = |\theta_{FN,left} - \theta_{FN,right}| \tag{16}$$

$$= \left|\cos^{-1}\left(-\frac{\lambda}{Nd}\right) - \cos^{-1}\left(\frac{\lambda}{Nd}\right)\right| \tag{17}$$

$$\approx \left|\frac{\pi}{2} + \frac{\lambda}{Nd} - \left(\frac{\pi}{2} - \frac{\lambda}{Nd}\right)\right| = \frac{2\lambda}{Nd} \tag{18}$$

where the approximation holds for long arrays, $L = Nd >> \lambda$.

3. The number of sidelobes increases as N is increased. In one period of $|f(\psi)|$ there are $N-2$ sidelobes.
4. The width of these minor lobes (in terms of ψ) is $2\pi/N$. The width of the major lobe is twice that.
5. The sidelobe level (SLL) decreases with N.
6. $|f(\psi)|$ is symmetric about $\psi = 0$ for $\psi = -\pi \ldots \pi$.

Example: $N = 2, d = \lambda$.

Let's try plotting the 2-element pattern using the technique just described. Note $kd = 2\pi$.

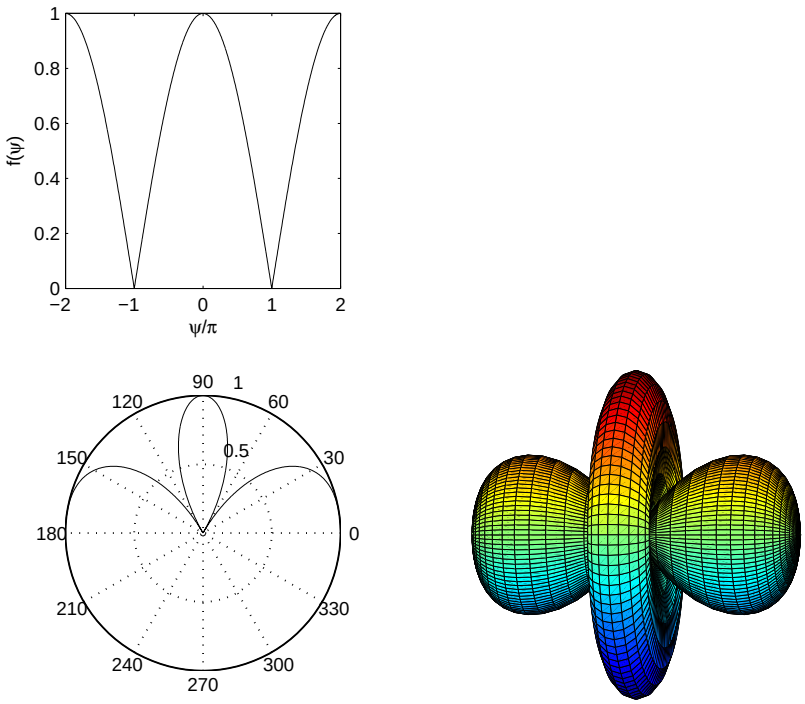

Figure 5: Pattern construction for $N = 2$, $d = \lambda$

Note that with this technique we plot what looks like "half" the pattern from $\theta = 0 \ldots \pi$. Technically, these are the bounds of theta, and the plot has been produced in a plane $\phi = 0^\circ$ in front of the array. To plot the response "behind" the array, we would need to consider a plane $\phi = 180^\circ$, but since we are considering isotropic radiators here, obviously the pattern will be symmetric. Hence, the 3-D pattern shown can be found by revolving the 2-D pattern about the z-axis.

From the resulting pattern we can see we have a combination of a broadside and a so-called *end-fire* pattern. End-fire patterns produce radiation along the axis of the array, which contrasts to normal to the axis for broadside patterns. Usually, we want a broadside pattern, or and end-fire pattern, or something in between, but not usually both. In fact, the end-fire lobes here are not desired and are called *grating lobes*. If you were to compute the directivity of such an array, it would not be very high since the pattern is quite unfocused.

Example: $N = 5, d = \frac{\lambda}{2}$.

Here, we have a strongly directive, broadside pattern: at $\theta = 90^\circ$, $|AF| = 5$ which improves our signal strength by a factor of $D = 5$. The sidelobes are very low. This pattern is very useful for focusing energy to/from a certain direction, and is called a *pencil beam* because of the shape of the pattern.

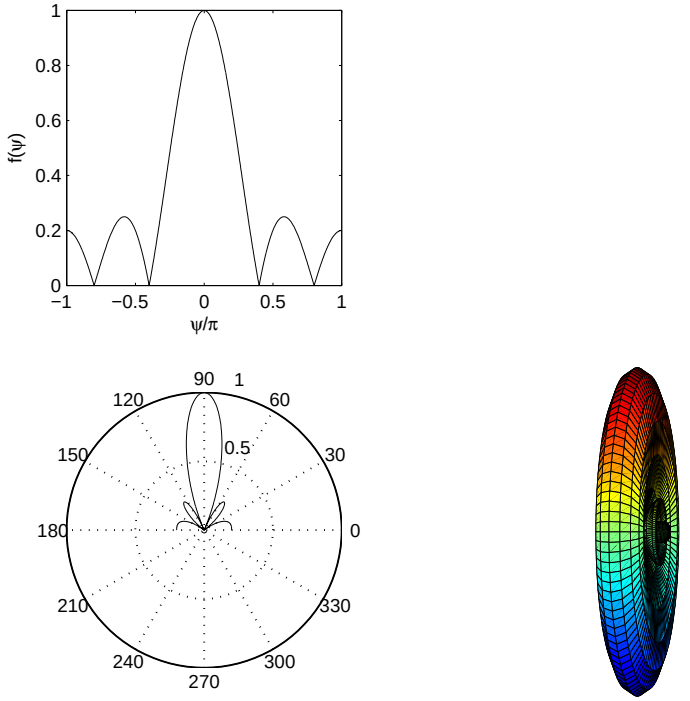

Figure 6: Pattern construction for $N = 5$, $d = \lambda/2$

2.1 Directivity of a Broadside Linear Array

The maximum directivity (which occurs in the broadside direction) of a uniformly excited ESLA can be found as follows. First, the normalizedarray factor is

$$(AF)_n = \frac{\sin(\frac{N}{2}kd\cos\theta)}{N\sin(\frac{1}{2}kd\cos\theta)}. \tag{19}$$

If $d \ll \lambda$, we can employ the small angle approximation for the denominator, yielding

$$(AF)_n \approx \frac{\sin(\frac{N}{2}kd\cos\theta)}{\frac{N}{2}kd\cos\theta}. \tag{20}$$

The normalized radiation intensity produced by this array factor is

$$U(\theta) = [(AF)_n]^2 = \left[\frac{\sin(\frac{N}{2}kd\cos\theta)}{\frac{N}{2}kd\cos\theta}\right]^2. \tag{21}$$

The average radiation intensity is found using

$$U_0 = \frac{P_{rad}}{4\pi} = \frac{1}{4\pi}\int_0^{2\pi}\int_0^{\pi}\left[\frac{\sin(\frac{N}{2}kd\cos\theta)}{\frac{N}{2}kd\cos\theta}\right]^2 \sin\theta d\theta d\phi, \tag{22}$$

which can be evaluated by making the subsitution

$$Z = \frac{N}{2}kd\cos\theta \Rightarrow dZ = -\frac{N}{2}kd\sin\theta d\theta \Rightarrow \sin\theta d\theta = -\frac{2}{Nkd}dZ. \tag{23}$$

This yields

$$U_0 = -\frac{1}{2}\frac{2}{Nkd}\int_{Nkd/2}^{-Nkd/2}\left[\frac{\sin Z}{Z}\right]^2 dZ. \tag{24}$$

If the array is very long (Nkd very large), then we can approximate U_0 as

$$U_0 \approx \frac{1}{2}\frac{2}{Nkd}\underbrace{\int_{-\infty}^{\infty}\left[\frac{\sin Z}{Z}\right]^2 dZ}_{\pi}, \tag{25}$$

since the integrand tends to zero for large Nkd values. The integral evaluates to π as shown, so

$$U_0 \approx \frac{\pi}{Nkd}, \tag{26}$$

and

$$D = \frac{U_{max}}{U_0} = \frac{1}{U_0} = \frac{Nkd}{\pi} = 2\frac{Nd}{\lambda}. \tag{27}$$

This result assumes the array length $L = Nd$ is very long ($L = Nd >> \lambda$). Note that for a special case of half-wavelength spacing,

$$D = N \tag{28}$$

and the directivity is simply equal to the number of elements in the array. Remember that this is the result for an array of isotropic radiatiors (i.e., the array factor), and that the incorporation of real elements (via pattern multiplication) will increase the overall directivity of the array.

3 Different Array Excitations

One of the biggest advantages of antenna arrays as that they allow many different array patterns to be synthesized. We have considered only one case so far, where each element is excited with an identical signal. Obviously, this does not necessarily need to be the case. Though we won't this situations much in this course, it is good to be aware of it and how it affects the radiation pattern.

We can introduce arbitrary element excitation by re-writing the array factor expression as

$$AF = I_0 + I_1 e^{jkd\cos\theta} + I_2 e^{jk2d\cos\theta} + \cdots I_{N-1}e^{jk(N-1)d\cos\theta} \tag{29}$$

$$= \sum_{m=0}^{N-1} I_m e^{jkmd\cos\theta} \tag{30}$$

Linear Phase Progression Between Elements

One very simple and useful case is where the magnitudes of all the element signals are the same ($|I_0| = |I_1| = |I_2| = \cdots = |I_{N-1}|$), which we will arbitrarily set to 1, but there is a progressive phase shift α between elements. Hence, we write the element excitation as

$$I_m = e^{jm\alpha} \tag{31}$$

Hence,

$$AF = \sum_{m=0}^{N-1} e^{jkmd\cos\theta + jm\alpha} \tag{32}$$

and redefining $\psi = kd\cos\theta + \alpha$, we can plot the array pattern using the graphical technique we studied already since $AF = \sum_{m=0}^{N-1} e^{jm\psi}$. We plot $f(\psi)$ for $\alpha = 0$, and to account for the inter-element phase shift, the circle $\psi = kd\cos\theta$ is shifted from the origin by an amount α. This is shown in Figure 3 for the 2-element $d = \lambda/2$ case discussed earlier.

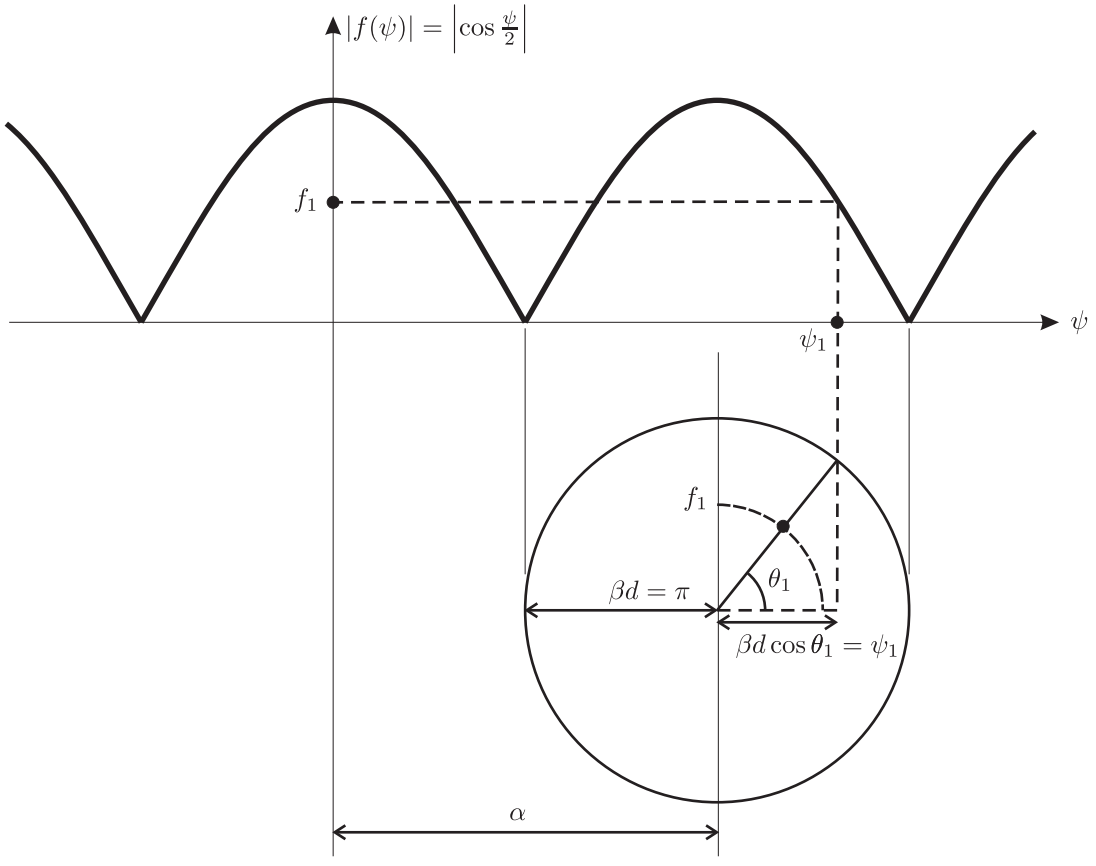

Figure 7: Geometric AF construction technique for $\alpha \neq 0$

The effect of this *linear phase gradient* is to *steer* the beam away from broadside (which is when $\alpha = 0°$). As an example, let's consider the 5 element case we discussed earlier, for various values of α. Figure 3 show the visible region of $|f(\psi)|$ with the pattern drawn below.

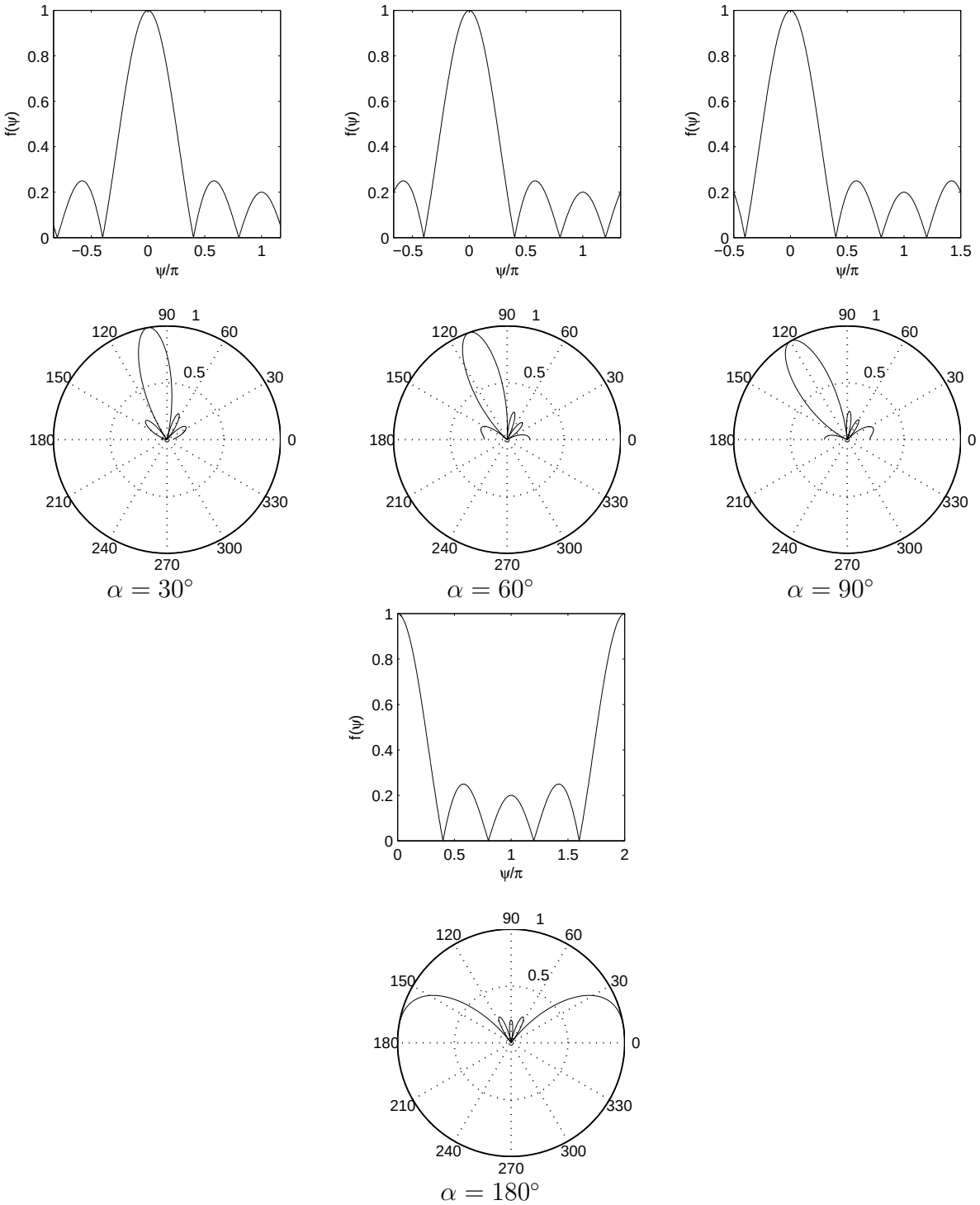

Figure 8: AF constructions for various values of α

Clearly the scanning action of the array is observable. In fact, if $\alpha = 180°$, the beam resembles an end-fire pattern with beams at $\theta = 0°, 180°$. This is highly useful behaviour because the beam of the array can be scanned without mechanically turning the antenna array; instead, electronic phase shifters can be introduced into the element paths and used to produce the phase gradient across the array to point the beam in the desired direction.

Amplitude Weighting

In addition introducing phase shift between elements to scan the beam, different amplitudes can be applied to the elements as well. We will not discuss this case in detail in this course. The graphical technique cannot be used in this case and the AF must be plotted directly using Equation (30), noting that

$$I_m = A_m e^{jm\alpha} \tag{33}$$

represents the element excitation if the linear phase gradient across the array is preserved.

The most common technique is to introduce an amplitude taper across the array to help reduce sidelobe levels, at the expense of a small reduction in the overall array directivity. Some examples of amplitude tapers are shown in Figure 9, and the corresponding impact on the array factor shown in Figure 10. Notice how all forms of tapering reduce the sidelobe level as at the expense of increasing the main lobe beamwidth (or decreasing the directivity of the array). That is, the best possible directivity of a broadside array occurs when there is *no tapering* across the elements (a). A simple triangular taper (b) reduces the sidelobes significantly, with the first sidelobe still being the strongest. Sidelobes can be eliminated altogether using a Binomial distribution (c) at the expense of a very wide main lobe. Finally, all the sidelobes can be set to be the same level in the case of a Dolph-Chebyshev array, for example, -20 dB relative to the main lobe (d) or -30 dB (e). While the synthesis of such arrays is beyond the scope of this course, we see that any reduction in the *effective usage* of the array results in lower directivities but better sidelobe levels.

4 Generalized Array Factor

So far, we have restricted our discussion to linear arrays, and in that analysis by itself, we have been assuming uniform spacing between elements. The more general form of the array factor expression is found using the following expression:

$$AF(\theta, \phi) = \sum_{M=1}^{N-1} I_m e^{j(k\hat{r}\cdot \boldsymbol{r}'_m)}, \tag{34}$$

where $\vec{r}'_m$ is a position vector to the mth element, and $\hat{r}$ is a unit vector pointing in the direction of interest, i.e.,

$$\hat{\boldsymbol{r}} = \sin\theta\cos\phi\,\hat{\boldsymbol{x}} + \sin\theta\sin\phi\,\hat{\boldsymbol{y}} + \cos\theta\,\hat{\boldsymbol{z}}. \tag{35}$$

I_m is the complex amplitude of the excitation of the mth element.

We note that for a linear, uniformly spaced array along the z axis, $\boldsymbol{r}'_m = md\,\hat{\boldsymbol{z}}$, yielding

$$\hat{\boldsymbol{r}}\cdot\boldsymbol{r}'_m = (\sin\theta\cos\phi\,\hat{\boldsymbol{x}} + \sin\theta\sin\phi\,\hat{\boldsymbol{y}} + \cos\theta, \hat{\boldsymbol{z}})\cdot md\hat{\boldsymbol{z}} = md\cos\theta, \tag{36}$$

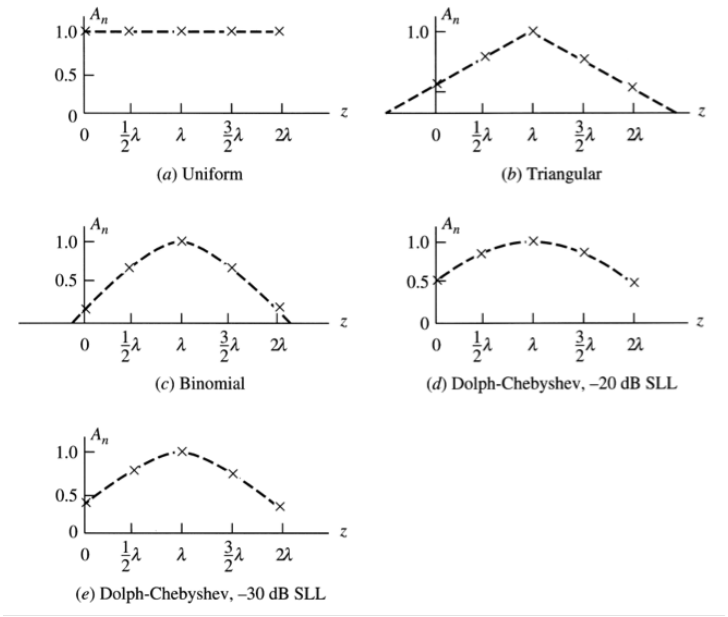

Figure 9: Amplitude tapers

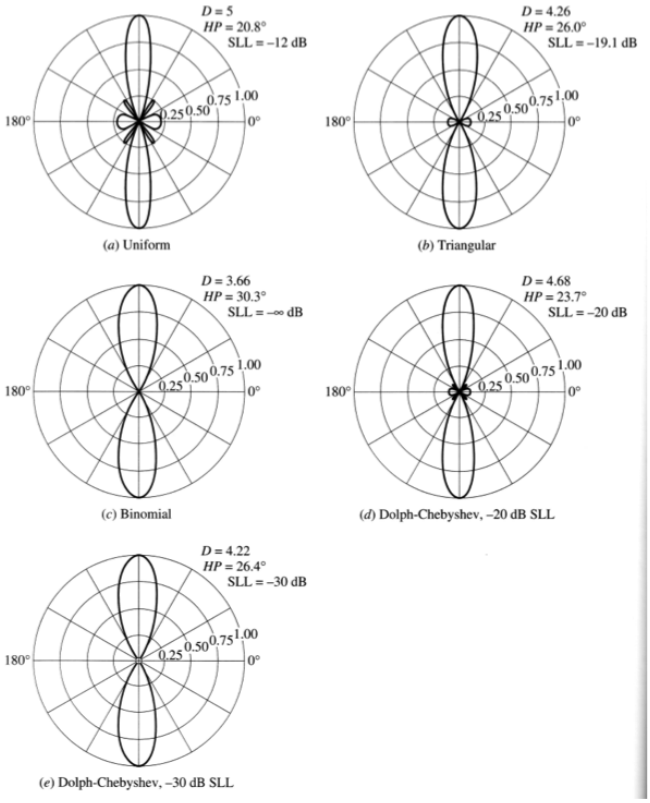

Figure 10: $|AF|$ patterns for various amplitude tapers

which when used in the generalized AF expression, gives

$$AF = \sum_{m=0}^{N-1} e^{jkmd\cos\theta}, \tag{37}$$

a familiar result.

We now use this array factor to derive the response of a few new array topologies.

4.1 Uniformly Spaced Linear Array Along Other Cardinal Directions

We can easily write array factors for linear arrays along other cardinal directions besides the z-direction by using an appropriate expression for the position vector $\vec{r}'_m$. For example, for an evenly spaced array along the x-axis,

$$\boldsymbol{r}'_m = md\,\hat{\boldsymbol{x}} \tag{38}$$

and

$$AF(\theta,\phi) = \sum_{m=0}^{M-1} I_m e^{jkmd\sin\theta\cos\phi}. \tag{39}$$

Notice that the AF is now a function of both θ and ϕ. Graphical techniques introduced earlier can also be applied to uniformly excited arrays, since the array factor often takes the general form

$$f(\zeta) = f(kd\cos\gamma + \delta) \tag{40}$$

where $\cos\gamma = \hat{\boldsymbol{r}}' \cdot \hat{\boldsymbol{r}}$ is the dot product between the array axis direction and the direction of interest, and δ is the inter-element phase shift. The normalized array factor is then

$$f(\zeta) = \left|\frac{\sin(N\zeta/2)}{\sin(\zeta/2)}\right| \tag{41}$$

which can be plotted using the following procedure:

1. Plot $f(\zeta)$ on a rectilinear graph with $\delta = 0$.
2. Draw a circle of radius kd below the graph, whose centre is offset from the origin ($\zeta = 0$) by an amount δ.
3. Vertical lines can be drawn between points of interest in $f(\zeta)$ and the circle to determine the corresponding polar pattern angles γ of these features.
4. $f(\zeta)$ can be evaluated at several points around the polar graph and the points connected to form the pattern.

Note that making such plots, as usual, requires one to define a cut in which one of θ or ϕ is kept constant while the other variable is varied over an appropriate range. This leads to the following cases:

Array along x-axis:

$$k\hat{r} \cdot \boldsymbol{r}'_m = md \sin\theta \cos\phi, \quad \psi = kd \sin\theta \cos\phi \tag{42}$$

- xy-cut: $\theta = 90°$, $\psi = kd\cos\phi$. This is similar to the result for an array along the $z-axis$ but with a $\cos\phi$ instead of a $\cos\theta$. Therefore, one can graphically construct the pattern in the same way as for an array along the z-axis, but intepret the physical angle as ϕ instead of θ.
- xz-cut: $\phi = 0$, $\psi = kd\sin\theta$. This is similar to the result for an array along the $z-axis$ but with a $\sin\theta$ instead of a $\cos\theta$. Therefore, the pattern must also be rotated 90 degrees after the construction process, since $\sin(\theta) = \cos(\theta - \pi/2)$.

Array along y-axis:

$$k\hat{r} \cdot \boldsymbol{r}'_m = md \sin\theta \sin\phi, \quad \psi = kd \sin\theta \sin\phi \tag{43}$$

- xy-cut: $\theta = 90°$, $\psi = kd\sin\phi$. This is similar to the result for an array along the $x-axis$ but with a $\sin\phi$ instead of a $\cos\phi$. Therefore, the pattern is versus ϕ and must be rotated $90°$ after its construction.
- yz-cut: $\phi = 90$, $\psi = kd\sin\theta$. This is similar to the result for an array along the $z-axis$ but with a $\sin\theta$ instead of a $\cos\theta$. Therefore, the pattern must also be rotated 90 degrees after the construction process.

4.2 Uniformly Spaced Planar Array

An example of a 2D planar array is shown in Figure 4.2. The elements are arranged uniformly along a rectangular grid in the xy-plane, with an element spacing d_x in the x-direction and an element spacing d_y in the y-direction.

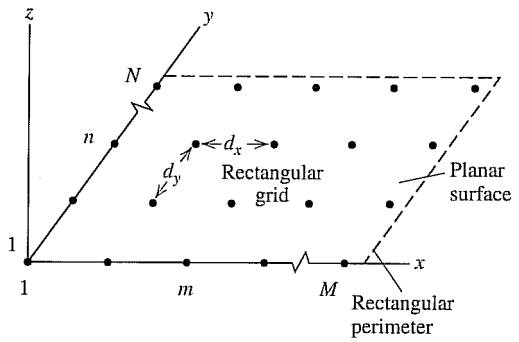

Figure 11: Two-dimensional planar array

Since the arrangement is Cartesian, or matrix-like, it is useful to use two indices to refer to the elements: a row index and a column index. Grid indices in the x and y direction are denoted as m and n, respectively. The position vector of the mnth element is then given by

$$\vec{r}'_{mn} = x'_{mn}\,\hat{\boldsymbol{x}} + y'_{mn}\,\hat{\boldsymbol{y}} + z'_{mn}\,\hat{\boldsymbol{z}} \tag{44}$$

Assuming we have the spacings indicated, and the array starts at the origin, we can rewrite the position vector as

$$\boldsymbol{r}'_{mn} = md_x\,\hat{\boldsymbol{x}} + nd_y\,\hat{\boldsymbol{y}} \tag{45}$$

where $m, n = 0, 1, 2, \ldots$. The array factor expression is then written as follows, where we have split the summation into two summations along each dimension:

$$AF(\theta,\phi) = \sum_{n=0}^{N-1}\sum_{m=0}^{M-1} I_{mn} e^{jk(md_x \sin\theta\cos\phi + nd_y \sin\theta\sin\phi)} \tag{46}$$

Here, I_{mn} denotes the excitation amplitude of the mnth element of the array, and is assumed to be a real number yielding broadside radiation.

The array factor is said to be *separable* if the excitations are such that

$$I_{mn} = I_{mx} I_{yn}. \tag{47}$$

That is, the excitation is the product of two functions, one describing variation in the x-direction and the other, the y-direction. Most commonly, we use uniform amplitude but progressive phase shifts in each direction such that

$$I_{mx} = I_0 e^{jm\alpha_x} \tag{48}$$

$$I_{yn} = I_0 e^{jn\alpha_y}, \tag{49}$$

where α_x and α_y are the phase gradients in the respective directions. Then,

$$AF(\theta,\phi) = I_0 \sum_{m=0}^{M-1} e^{jk(md_x \sin\theta\cos\phi + \alpha_x)} \sum_{n=0}^{N-1} e^{jk(nd_y \sin\theta\sin\phi + \alpha_y)}, \tag{50}$$

which we see is simply the product of two linear array factors. This means that the beamwidths in each of the principal directions of the array will be determined by a linear array along the corresponding direction.

4.3 Circular Arrays

A circular array is another arrangement that is commonly found in phased arrays and recently, microwave beacon arrays. A general diagram of a circular array is shown in Figure 4.3 for a 8-element array, although any number of elements is possible. The radius of the array is a. The angle between elements is assumed to be uniform, such that

$$\Delta\phi = \phi_{n+1} - \phi_n = \frac{2\pi}{N}. \tag{51}$$

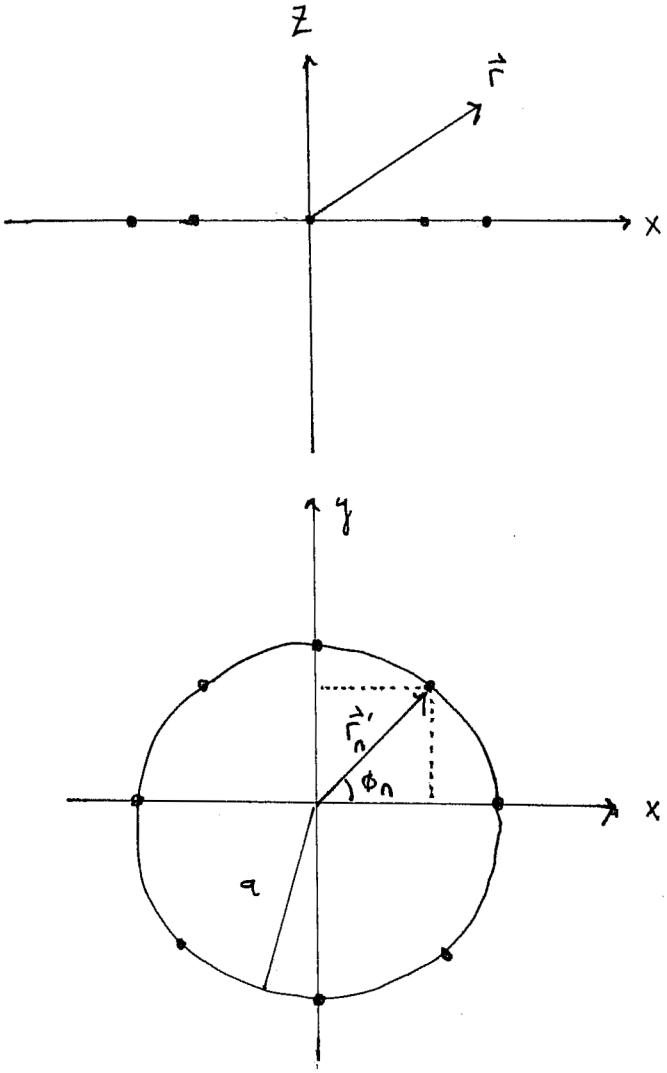

Figure 12: Circular array

If this is the case, the position vector of the nth element can be written as

$$\boldsymbol{r}'_n = a\cos\phi_n\,\hat{\boldsymbol{x}} + a\sin\phi_n\,\hat{\boldsymbol{y}} \tag{52}$$

where

$$\phi_n = n\Delta\phi = \frac{2\pi}{N}n \tag{53}$$

The corresponding array factor expression is

$$AF = \sum_{n=0}^{N-1} I_n e^{jka[\cos(2\pi n/N)\sin\theta\cos\phi + a\sin(2\pi n/N)\sin\theta\sin\phi]} \tag{54}$$

5 Feeding Array Antennas

There are a variety of ways to excite array antennas, depending on what the characteristics in the array are desired. Generally, transmission lines must be run to each and every antenna element. The amplitude and phase of the element excitations can be varied using discrete amplitude/phase shifting devices, or the feed network, or a combination of both. A sampling of some common feed networks are shown in Figure 5.

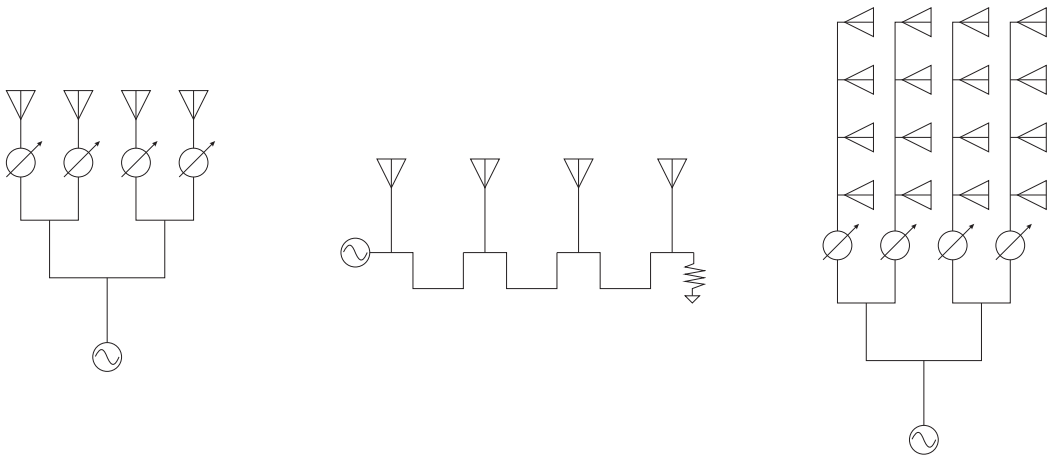

Parallel or corporate feed Series feed Hybrid feed

Figure 13: Array feeds

In a *parallel* or *corporate* feed network, all the elements are feed in parallel from a single source. Practically, the power splitters are realized using special RF power dividers, such as Wilkinson power dividers, or lossless combiners. Tricks can often be employed to combine matching and power division in the feed network; for example, instead of tuning the antenna to 50 Ω, it can be tuned to 100 Ω and two antenna combined in parallel using a lossless combiner to produce a 50 Ω input impedance to a 2-element sub-array. In any case, at the antenna level, phase and/or amplitude shifters can be added to control the element excitations, allowing a wide variety of patterns and/or beam scanning to be introduced to the array.

In a series-fed array, antennas are feed in series from a common source. As the signal travels away from the source, antennas tap off the power, which usually results uneven power distribution to the antennas that must be accounted for in array factor calculations. The inter-element phasing is controlled by changing the length of feed line between the elements; for example, choosing a length equal to one wavelength will result in all elements being fed in phase. An advantage of this type of array structure is that it implements something called *frequency scanning*, since the beam will scan with frequency. For example, using the one wavelength example, all the element will be in phase at the frequency where the feed-line lengths are one wavelength. However, when the frequency changes, the electrical length of the transmission line changes, resulting in shortening (if the frequency is decreased) or lengthening (if the frequency is increased) of the feed-lines. This in turn changes the inter-element phase shift which we know causes the beam to tilt away from broadside. In some applications, this can be very useful. It is also quite easy to realize series-fed arrays, depending on the transmission line technology. Periodic radiating slots cut in a waveguide are an example.

Both concepts can be combined into a *hybrid* feed or parallel-series feed. Sub-arrays are formed as series-fed groups of elements, fed by a common signal from a parallel feed structure. The parallel structure in turn allows the individual amplitudes/phases of the sub-arrays to be controlled if necessary.